KfK 4310
September 1987

IVA 2 Verification Expansion Phase Experiment in SNR Geometry

N. I. Kolev
Institut für Neutronenphysik und Reaktortechnik

Kernforschungszentrum Karlsruhe

Kernforschungszentrum Karlsruhe

Institut für Neutronenphysik und Reaktortechnik

KfK 4310

IVA2 Verification

Expansion Phase Experiment in SNR Geometry

N.I. Kolev

Kernforschungszentrum Karlsruhe GmbH, Karlsruhe

Kernforschungszentrum Karlsruhe GmbH
Postfach 3640, 7500 Karlsruhe 1

ISSN 0303-4003

Abstract

Using the IVA2/005 computer code the SNR model explosion experiment SGI-09-1 was numerically simulated. The experiment consists of high pressure gas injection into a low pressure liquid pool with a free surface in a cylindrical geometry with internals. Bubble formation and pressure history as a function of time was predicted and compared with the experimental observation. A good agreement between theory and experiment was obtained. Numerical diffusion and its influence on the results are discussed.

IVA-2-Verification: Expansions-Phasen Experiment in SNR-Geometrie

Zusammenfassung

Mit Hilfe des Computerprogramms IVA2/005 wurde ein SNR Modell-Explosionsexperiment, mit der Nummer SGI-09-1, simuliert. Das Experiment bestand aus einer Hochdruckgasinjektion in einen Niederdruckbehälter, der teilweise mit Wasser gefüllt war. Experimentelle und theoretische Ergebnisse bezüglich der Blasenbildung und Druckwellenausbreitung wurden in Abhängigkeit von der Zeit verglichen und es wurde eine gute Übereinstimmung festgestellt. Anschließend wird auf die Problematik der numerischen Diffusion und deren Einfluß auf die Ergebnisse eingegangen.

Table of contents

1. Introduction
2. Short description of the experiment and discretisation scheme
3. Mathematical option used
4. Comparison theory-experiment
5. Timing
6. Conclusion
7. Acknowledgement
8. References

1. Introduction

Experience gained with small scale experiments can be made useful for the engineering practice in different ways. One of them, may be the most powerful today, is the mathematical modelling of a wide spectrum of differnt small and/or semi scale experiments with the same computer code, revealing the application limits and the accuracy of the modelling technique and having this in mind, using the code for practical engineering design. Following this philosophy, the computer code IVA2 was developed /1-5/ for the simulation of a large number of processes connected with transient three phase, three component flow in complicated industrial facilities by means of three velocity fields. As mentioned in /3/, the code can not yet be completed with the constitutive relations for every combination of flow pattern, velociy fields, phase and components becuase for some combinations either no empirical information is available or the available information is not complete. Nevertheless, the code architecture and the recent constitutive package allows modelling of a number of processes of technical interest. As a part of the verification procedure a comparison of the code prediction of the expansion experiments in SNR-typical geometry was made. This comparison allows to make interesting conclusions about the accuracy, performance and the limits of the modelling technique described in /3/, especially with respect to pressure wave propagation in a complicated geometry and with respect to a strong inhomogeneity of fluid phases.

The purpose of this paper is to present the results obtained by this comparison.

2. Short description of the experiment and discretisation scheme

The full description of the experimental facility, instrumentation and experimental procedure used are documented in /6/. We summarize here only the important initial and boundary conditions relevant for the computational simulation.

An axisymmetric vessel simulating SNR-typical geometry in 1:20 scale was used. Before starting the experiment the vessel was divided in a high (1.1 MPa) and a low (0.1 MPa) pressure region by means of sliding doors and an aluminum burst foil above them as shown in fig. 1. The high pressure region consists of nitrogen of 1.1 MPa. The low pressure region consists of degased water (air volumetric fraction = 0.002-0.005 typically) having a label given in Fig. 1 and air at 0.1 MPa

and room temperature. Using a sophisticated explosion technique the doors are opening within 0.0004 s. The pressure was measured in different positions shown in Fig. 1 and marked by (p). Two high speed film cameras (90 deg from each other, 7 pictures per millisecond) were used to record the bubble growth region. We chose the experiment with number SGI-09-1 /6/ for this simulation.

More references about the past of these experiments can be found in /7/. Note that in /7/ the theoretical prediction of the SIMMER-II computer code was compared with the experimental results of the previous sequence of similar experiments but with a dip plate. The experiments performed by Meyer and Kirstahler without a dip plate were simulated for the first time with the IVA2 computer code. Computational simulation assumes a symmetrical process, neglecting the inevitable small asymmetry measured in /6/. The geometry was presented by 9 x 23 cells as shown in Fig. 1 in only one angular sector in cylindrical geometry.

3. Mathematical options used

The model as described in /3/ was used with the additional introduction of

- surface permeabilities as a function of time in order to simulate adequately the opening of the sliding doors and
- a vertical plane by plane solution of the Poisson equation.

Because of the observation experience of predominant acceleration in the initial phase, the entrainment in the sense of dividing the liquid into continuous and noncontinuous velocity fields was suppressed.

4. Comparison theory-experiment

Figure 2 shows the computed volumetric gas fraction as a function of the two dimension space (r,z) in the gas entrance region. The time is used as a parameter in the pictures a) through d). The experimentally observed sharp bubble boundary is also shown in the figures. The bubble boundary in the sense of the experimental observation divides a region of "pure" liquid from the two phase

region with predominant gas volumetric fraction. From these comparisons the following conclusions can be drawn:

1. With the first order discretisation of the mass conservation equation sharp bubble boundaries cannot be predicted.

2. In the sense that the bubble boundary is defined as the boundary between the region with predominant gas volumetric fraction and the region with predominant liquid volumetric fraction the coincidence between theoretical prediction and experimental observation is acceptable from an engineering point of view.

Figure 2 illustrates very clearly the physical meaning of the socalled "computational diffusion". The consequence of this phenomenon is the predistribution (smearing) of the momentum in the sharp boundaries of the bubble surface and of the liquid surface in the upper plenum, too. So one has to expect, that the impact of the liquid on the top will transfer mechanical energy not as a sharp pressure peak, but as a Gaussian-like pressure distribution as a function of time. This is exactly what we obtain from the numerical simulation.

Among the different measures which can be undertaken to come closer to the reality one has either

- to increase the number of the computational cells or

- to increase the order of the discretisation at least of the mass conservation equations.

Figures 3 shows the pressure on the top and bottom as a function of time as predicted by the IVA2 code. The space coordinates where the pressures are defined are given in Fig. 1.

An important phenomenon can be recognized from that picture - that is the way, how the mechanical enery is transferred from the axis to the outer vertical wall and reflected back from the wall. The stronger the initial impact on the top, the smaller the amplitude of the reflected wace because of the overall momentum conservation. This is the mechanism which explains how the "numerical diffusion" influences the computed pressure peak on the top.

Figure 4 shows the computed static pressure on the top - center line compared with the sum of the measured static plus dynamic pressures. The same, but for

the position (r = 0.686-0.699), is shown in Fig. 5. The following conclusions can be drawn from these pictures:

- The time, when the pressure peak occurs is predicted very well by IVA2.
- The difference in the amplitudes can be explained

  1) by the differences in the measured sum of the static plus dynamic pressures and the static pressure predicted by IVA2 and

  2) by the influence of the numerical diffusion as already mentioned above.

- The small secondary increase of the pressure at about 11 ms was experimentally recorded (not shown in figs. 4 and 5) but not with the amplitude predicted by IVA2, which has been already explained by the influence of the numerical diffusion.

Figure 6 shows the predicted static pressure on the top corner compared with the measured dynamic plus static pressure. In the same figure the predicted and measured pressure in the lower gas plenum is shown. We see a very good agreement between experimental and predicted data.

The small differences between the pressure maxima can be explained by the fact that the axial velocity component in that position is very small.

Figure 7 shows the predicted and measured static pressures in the inlet nozzle. Unfortunately, the pressure tap signal was cut by malfunction during the experiment below 0.6 MPa, maybe because a part of the broken foil was damping the signal of the pressure transducer, so that the comparison between 0.4 ms and 6 ms is not informative. But the agreement within the first 0.4 ms and after 6 ms is very good. The character of the predicted pressure on that position is supported by other experiments with different pressure sources /6/.

Figure 8a) through f) show the predicted liquid fraction as a function of (r,z) space. The time is used as a parameter. The first four figures correspond to Figs. 2a) through d). One can clearly see the erosion, deformation and displacement of the liquid as a function of time. The surface motion is also seen. Figure 8e) shows the liquid distribution in the space at a time a little bit later than the maximum static pressure on the top (center line) is reached. Figure 8f) shows the liquid distribution at the time when the maximum static pressure in the top

corner occurs. The corresponding distributions of the gas volumentric fraction are given in Figs.9a) through 9f).

Figures 10a) through 10d) reveal the mechanism of the pressure formation below the water surface. During the time before the bulk liquid reaches the top, the water surface reflects the pressure wave, so that the pressure increase in the region below the surface is the result of an interference of the waves arising from the pressure source from one side and the waves reflected from the internals and the water surface from the other side. The pressure above the surface is build in the first seven milli-seconds by the air compression because of the liquid surface motion. The evidence that the static pressure maximum on the top center line and top corner occurs when the accelerated bulk liquid is reflected from the walls is obvious from the comparison of the Figs.8 e-f) with the Figs. 10e-f), respectively. The compacter the bulk liquid the bigger the static pressure maximum and the smaller the impact time.

5. Timing

In order to suppress the numerical diffusion as far as possible for this number of cells we used the maximal possible time step of 200-50 s. The physical time of 11 ms is simulated by 14.57 min CPU time on a Siemens 7890 computer, tolerating an average mass error of 5% and using a printing frequency of 5-20 in order to resolve the pressure peaks.

6. Conclusion

From an engineering point of view the IVA2/005 computer code is able to predict realistic pressure wave phenomena in two-phase, two-component mixtures with substantial nonhomogeneity. The overall predictive capability of the pressure and gas fraction distributions is acceptable. The differences between theoretical prediction and experimetnal results with respect to sharpness of

- the bubble boundary,
- the liquid surface motion

and their influence on the pressure history is explained by the inevitable numerical diffusion. Reducing numerical diffusion by means of increasing the

number of mesh cells and/or increasing the order of the discretisation of the mass conservation equations can result in a prediction closer to reality.

7. Acknowledgement

I am deeply indepted to Prof. Rehme and Dr. Meyer for the motivation to perform this study and for the truthful discussions during my visit in KfK.

8. References

/1/ Kolev N.I.: Transient Three-Dimensional Three-Phase Three-Component Nonequilibrium Flow in Porous Bodies described by Three-Velocity Fields, Kernenergie 19(1986)10 pp.383-392 or in German in KfK 3910, März 1985.

/2/ Kolev N.I.: Transient three-phase three-component nonequilibrium nonhomogeneous flow described by a one-dimensional slip model. Atomkernenergie, Kerntechnik Vol. 49(1987)No.4, or in German in KfK 3926, August 1985.

/3/ Kolev N.I.: A three-field diffusion model of three-phase, three-component flow for the transient three-dimensional computer code IVA2/001, Nuclear Technology, to be published in August 1987, or in German in KfK 4080, Mai 1986.

/4/ Kolev N.I.: IVA2 - Ein Computerprogramm zur Modellierung transienter 3D-Dreiphasen Dreikomponenten Strömungen mittels drei Geschwindigkeits-feldern in zylindrischer Geometrie mit beliebigen Einbauten einschließlich der Spaltzone eines PWR/BWR, Kfk 4088 Juni 1986.

/5/ Kolev N.I.: Transiente Zweiphasen-Strömung, Springer-Verlag, Berlin, Heidelberg, New York, Tokyo 1986.

/6/ Meyer L., Kirstahler M.: SGI-09-1 experiment, 1987 to be published.

/7/ Küfner K., Schmuck P., Fröhlich R.: SIMMER-II Analyses of Expansion Phase Experiment in SNR Geometry, KfK 3639 Oktober 1984.

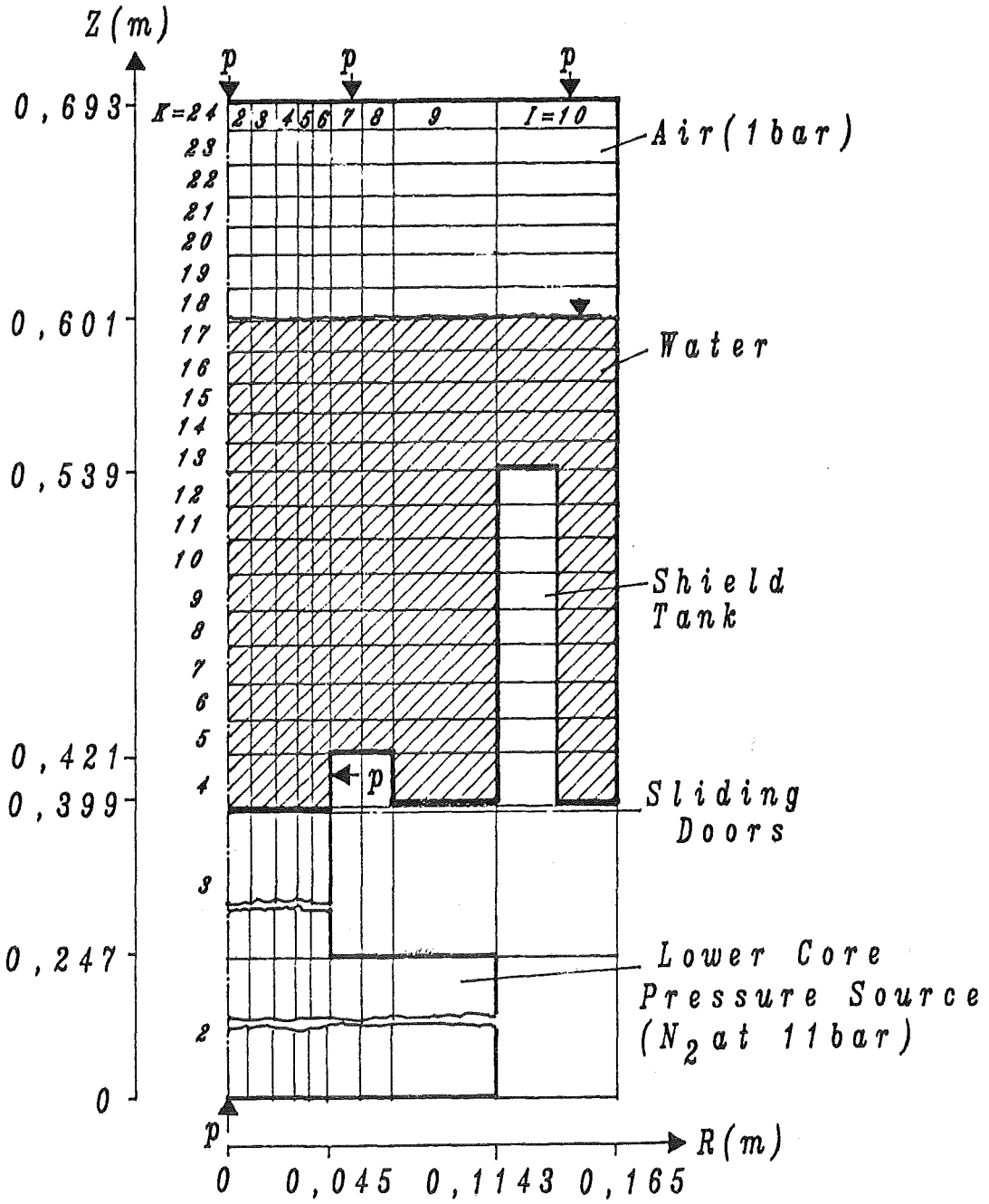

Fig. 1 IVA2/005-discretisation mesh and model of the Meyer-Kirstahler-experiment.

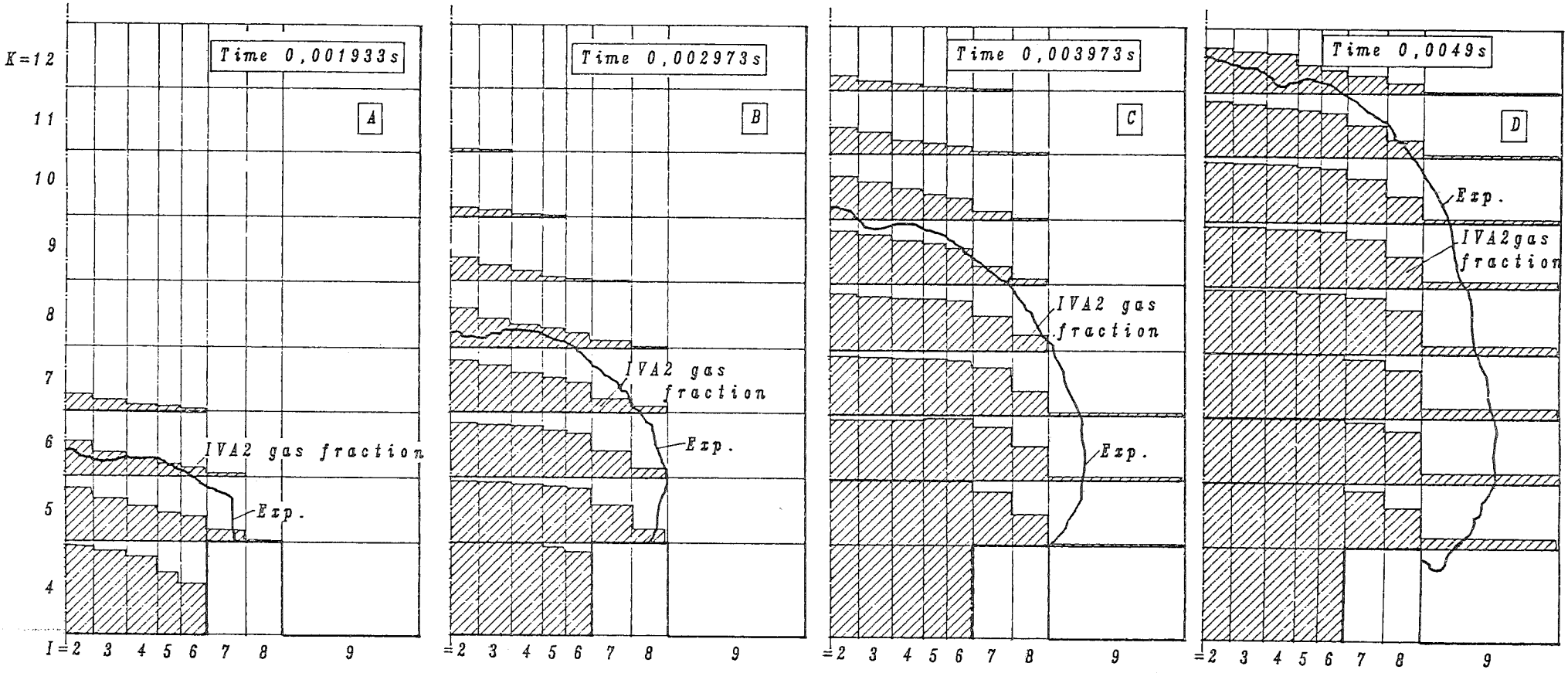

Fig.2 Bubble growth as a function of time. Comparison of IVA2/005 prediction with the Meyer-Kirstahler experiment.

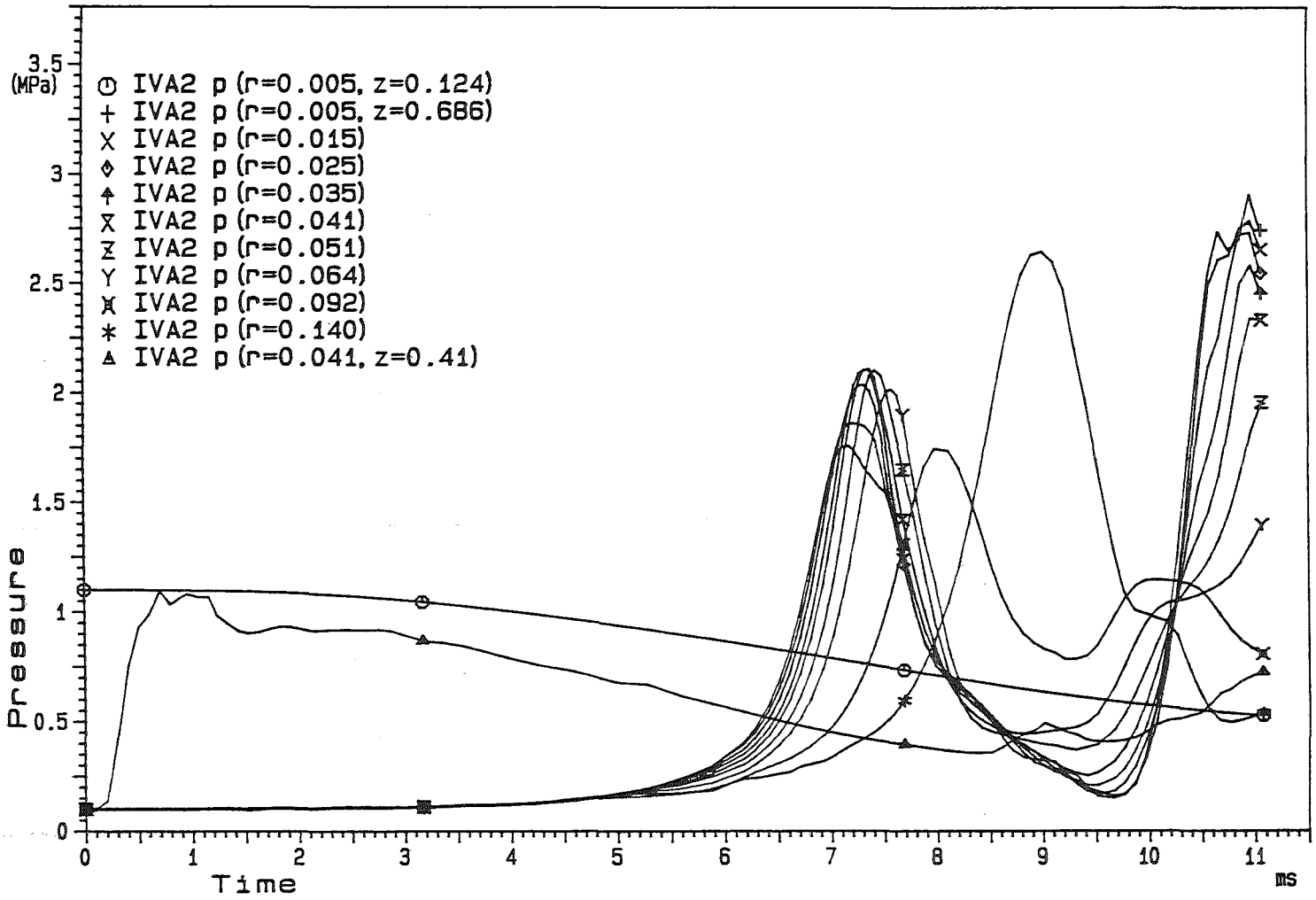

Fig.3 Pressure on the top and bottom as a function of time. IVA2/005 calculation of Meyer-Kirstahler SNR model explosion experiment [6]. Pressure source 1.1 MPa.

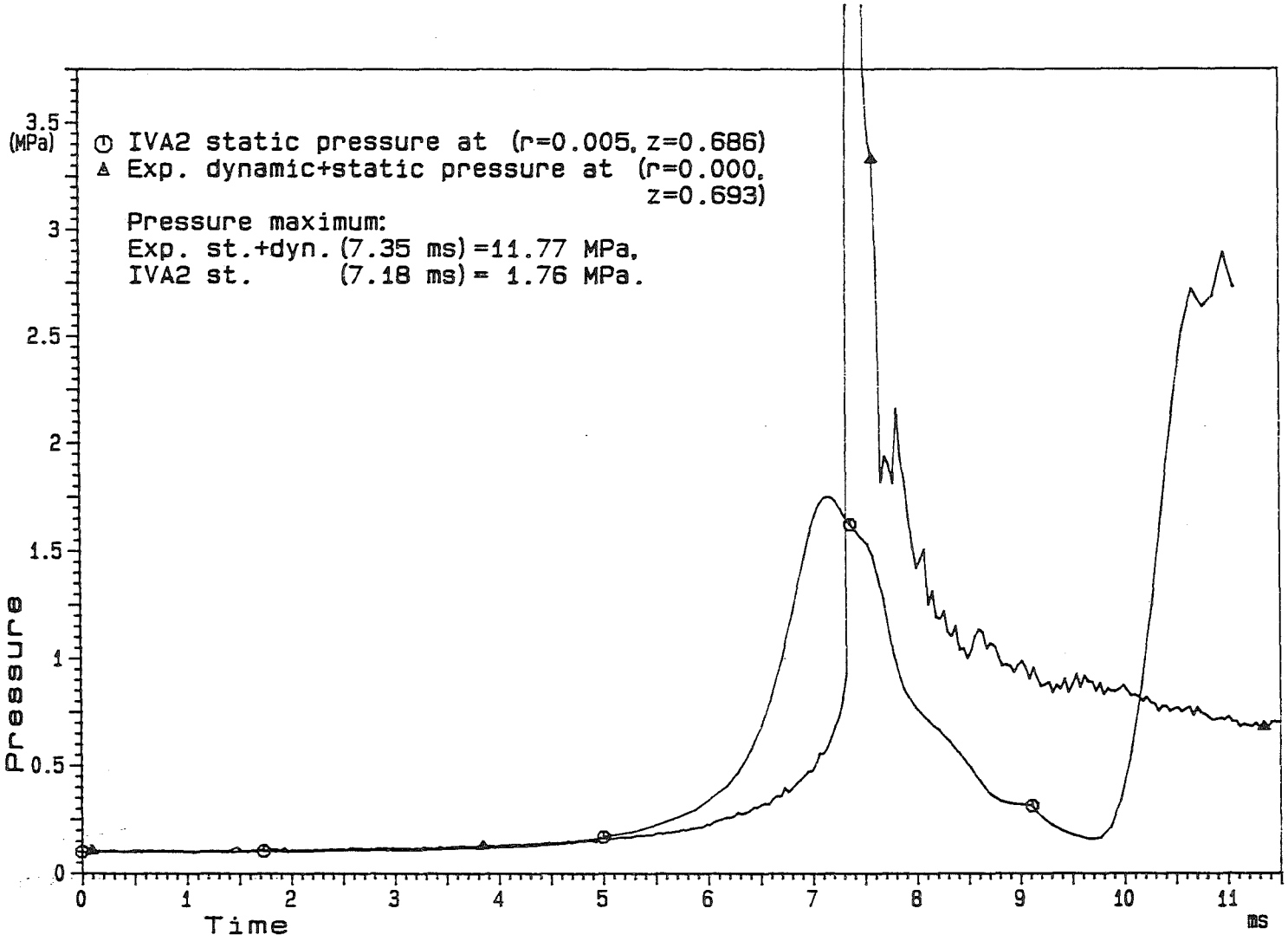

Fig.4 Pressure on the top as a function of time. Comparison of the IV2/005 prediction with Meyer-Kirstahler SNR model explosion experiment [6]. Pressure source 1.1 MPa.

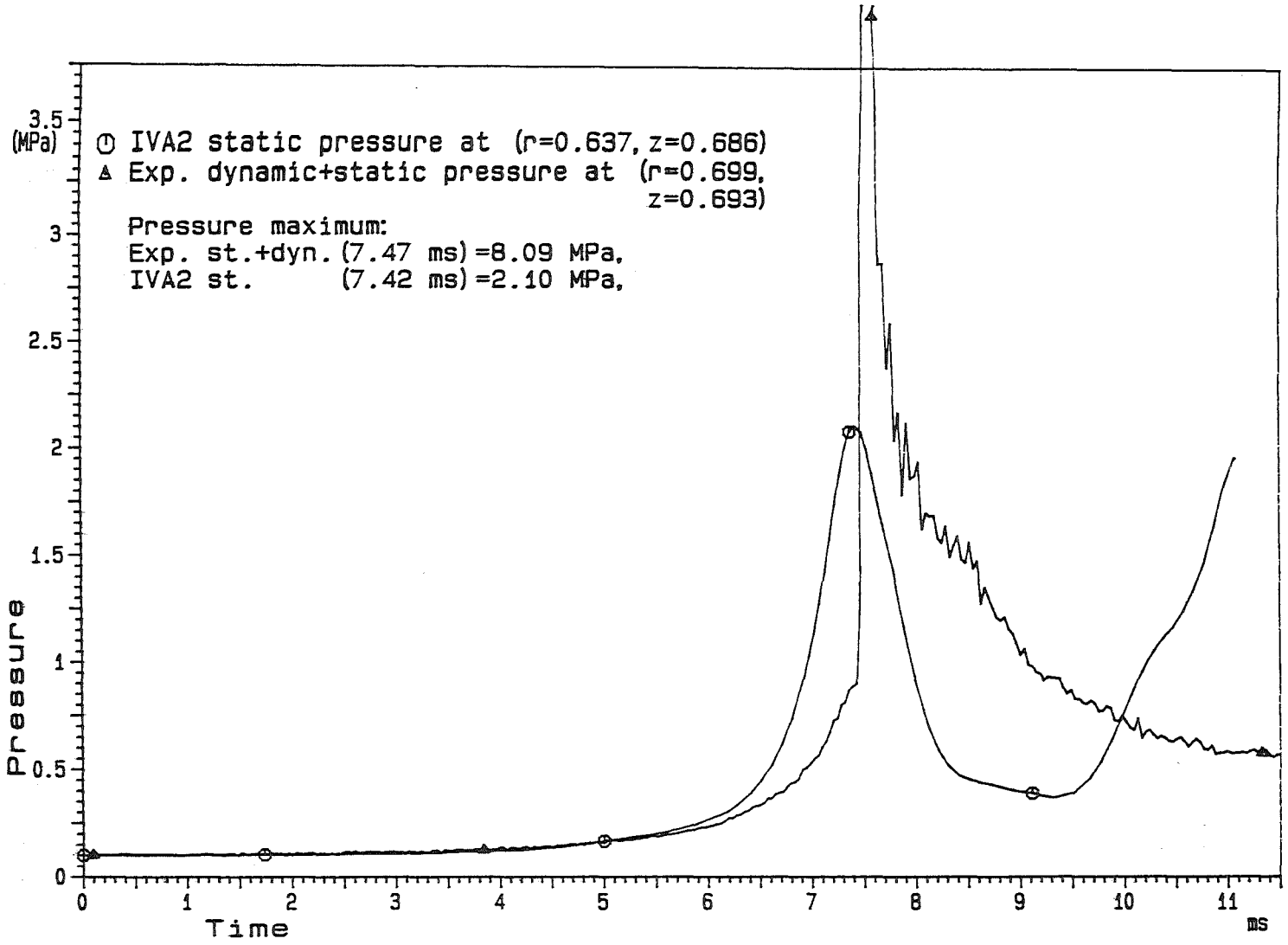

Fig.5 Pressure on the top as a function of time. Comparison of the IV2/005 calculation with Meyer-Kirstahler SNR model explosion experiment [6]. Pressure source 1.1 MPa.

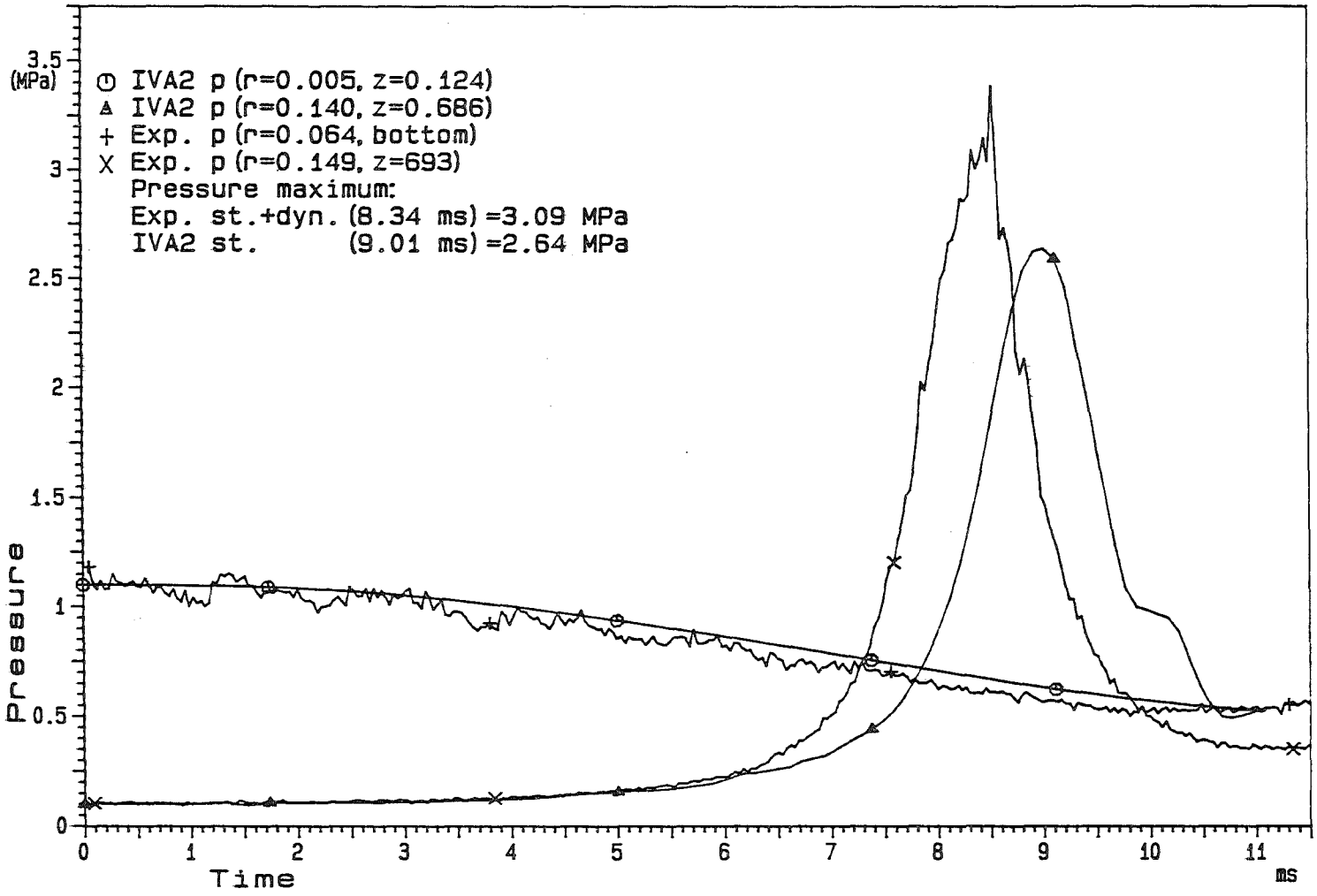

Fig.6 Pressure on the top corner and bottom as a function of time. Comparison of the IV2/005 prediction with Meyer-Kirstahler SNR model explosion experiment [6]. Pressure source 1.1 MPa.

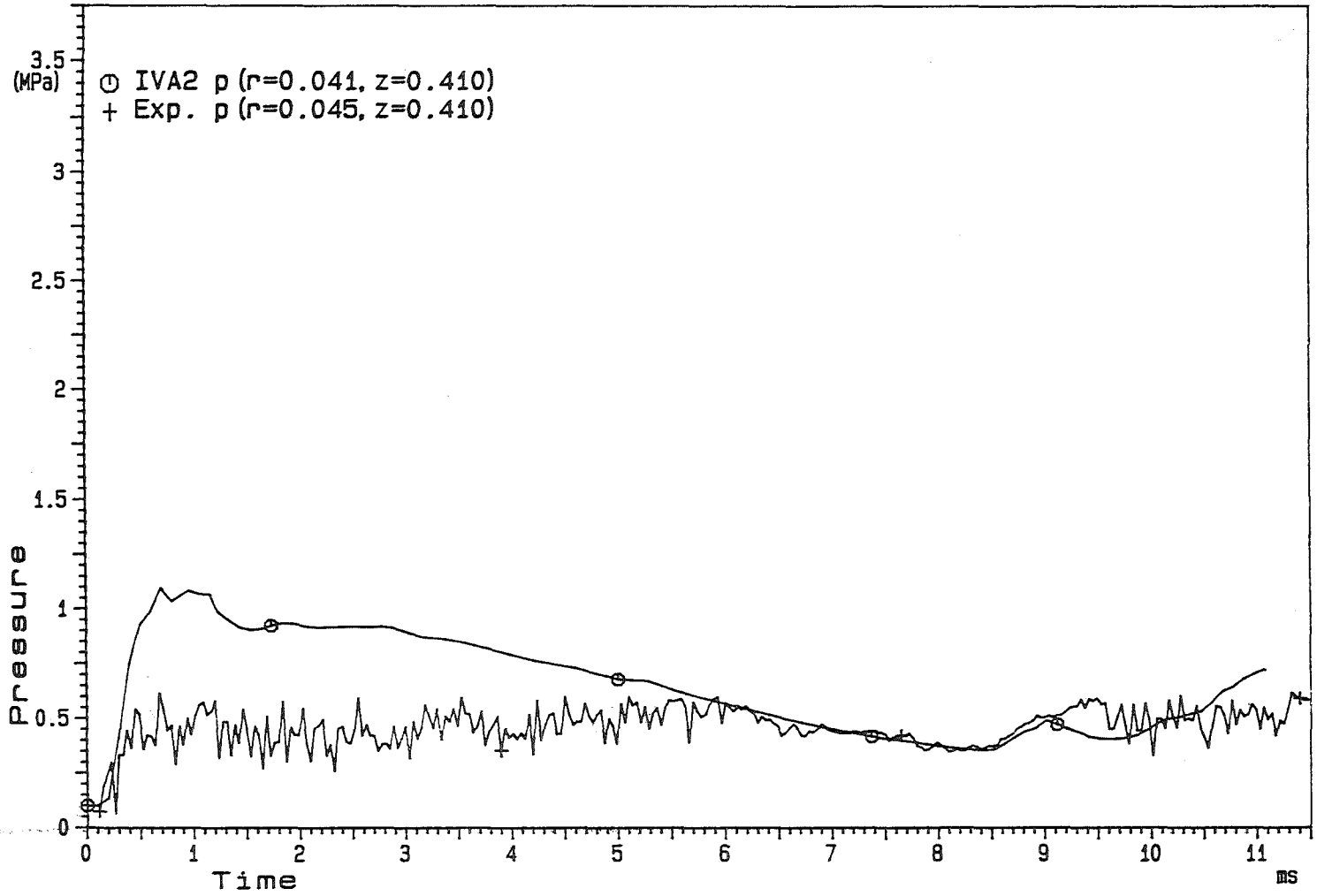

Fig.7 Pressure on the nozzle outlet as a function of time. Comparison of the IV2/005 prediction with Meyer-Kirstahler SNR model explosion experiment [6]. Pressure source 1.1 MPa.

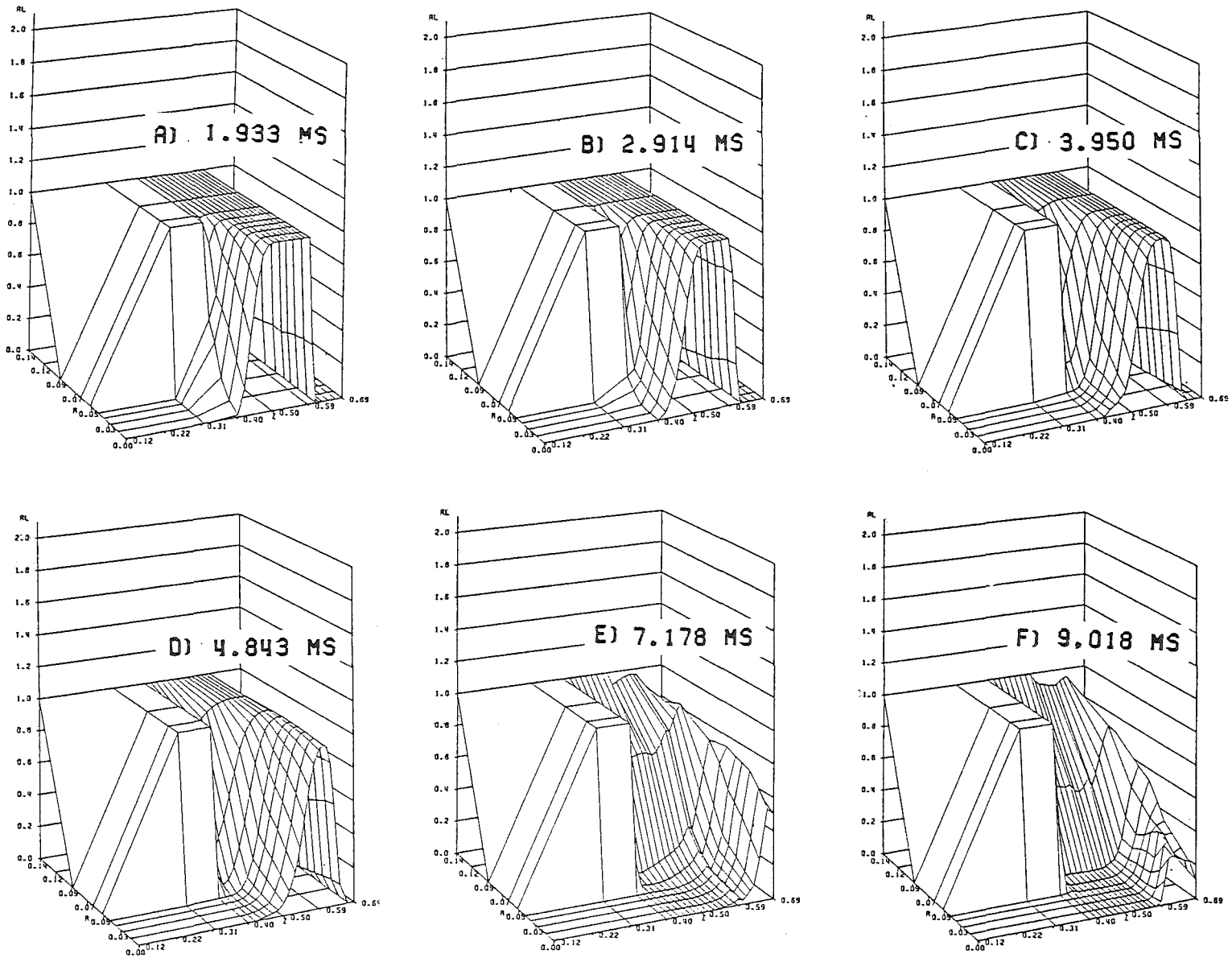

FIG.8 LIQUIDFRACTION AL2(-) J=2.

IVA2/005-VARIFICATION (SNR-MODEL ACCIDENT)

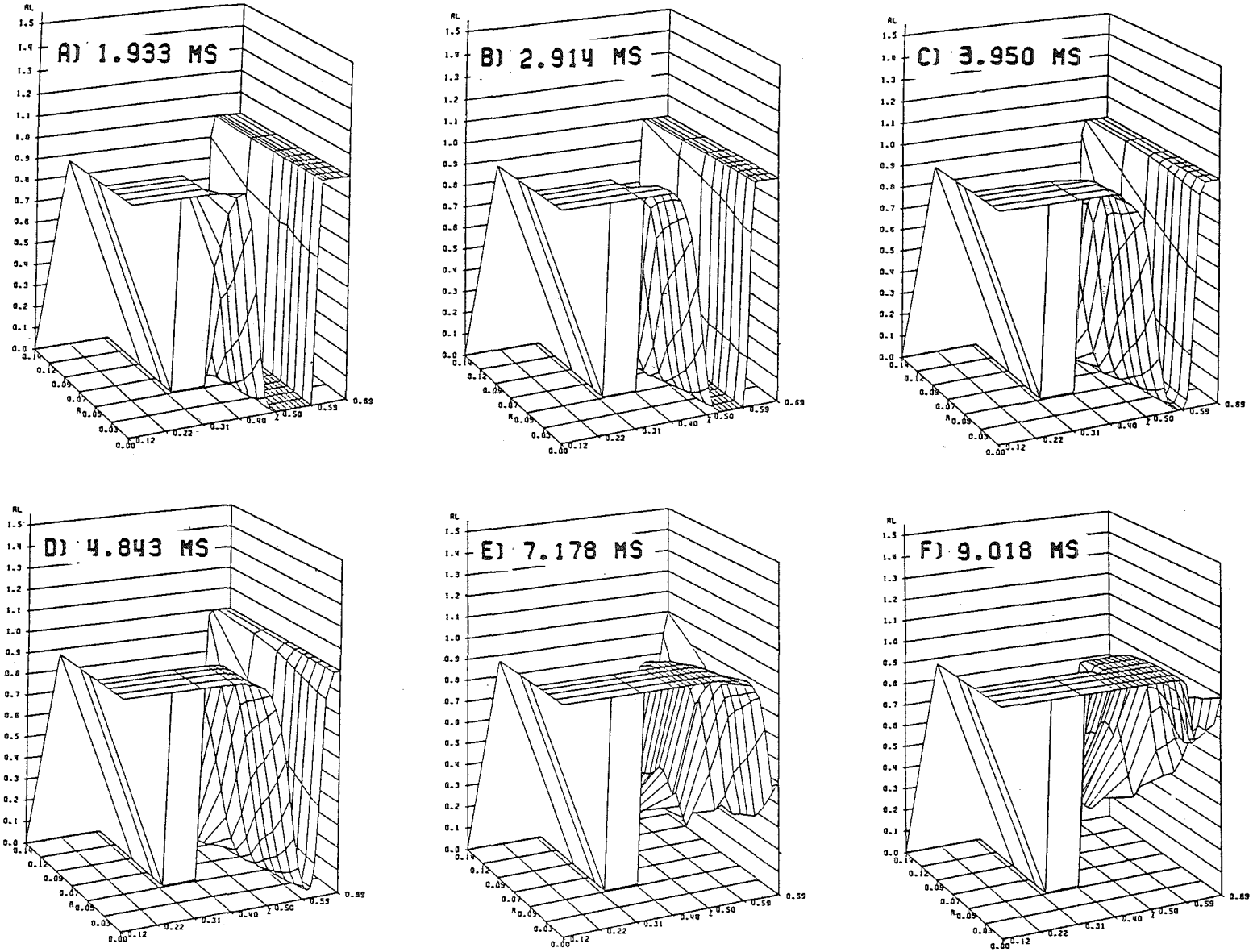

FIG.9 VOIDFRACTION AL1(-) J=2.

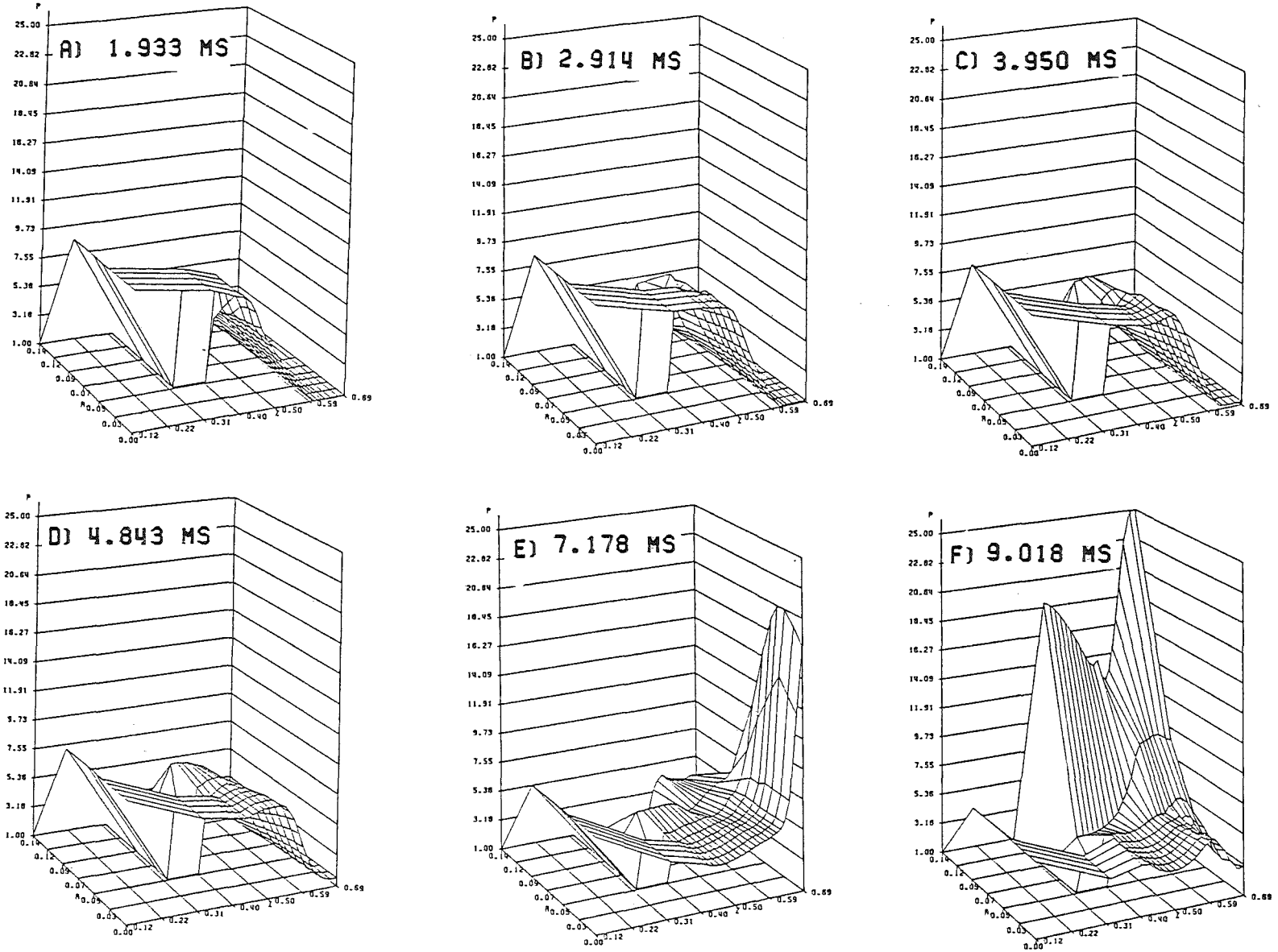

FIG.10 SPACE PRESSURE WAVE P(BAR) J=2.